

Joint Optimization of Fronthaul Compression and Bandwidth Allocation in Uplink H-CRAN with Large System Analysis

Wenchao Xia, Jun Zhang, Tony Q. S. Quek, Shi Jin, and Hongbo Zhu

Abstract

In this paper, we consider an uplink heterogeneous cloud radio access network (H-CRAN), where a macro base station (BS) coexists with many remote radio heads (RRHs). For cost-savings, only the BS is connected to the baseband unit (BBU) pool via fiber links. The RRHs, however, are associated with the BBU pool through wireless fronthaul links, which share the spectrum resource with radio access networks. Due to the limited capacity of fronthaul, the compress-and-forward scheme is employed, such as point-to-point compression or Wyner-Ziv coding. Different decoding strategies are also considered. This work aims to maximize the uplink ergodic sum-rate (SR) by jointly optimizing quantization noise matrix and bandwidth allocation between radio access networks and fronthaul links, which is a mixed time-scale issue. To reduce computational complexity and communication overhead, we introduce an approximation problem of the joint optimization problem based on large-dimensional random matrix theory, which is a slow time-scale issue because it only depends on statistical channel information. Finally, an algorithm based on Dinkelbach's algorithm is proposed to find the optimal solution to the approximate problem. In summary, this work provides an economic solution to the challenge of constrained fronthaul capacity, and also provides a framework with less computational complexity to study how bandwidth allocation and fronthaul compression can affect the SR maximization problem.

Index Terms

W. Xia, J. Zhang, and H. Zhu are with the Jiangsu Key Laboratory of Wireless Communications, Nanjing University of Posts and Telecommunications, Nanjing 210003, P. R. China, E-mail addresses: { 2015010203,zhangjun,hbz }@njupt.edu.cn.

T. Q. S. Quek is with the Singapore University of Technology and Design, Singapore 487372, E-mail address: tonyquek@sutd.edu.sg.

S. Jin is with the National Mobile Communications Research Laboratory, Southeast University, Nanjing 210096, P. R. China, E-mail addresses: jinshi@seu.edu.cn.

This work was presented in part at IEEE Global Communications Conference (GLOBECOM) [1], Singapore, Dec. 2017.

H-CRAN, fronthaul compression, compress-and-forward, Wyner-Ziv coding, point-to-point compression, bandwidth allocation, random matrix theory.

I. INTRODUCTION

With the development of the Internet of things and mobile communication networks, the demands for high-speed data applications are growing exponentially recently [2]. Meeting such challenging goals should involve new system architectures and advanced signal processing for wireless communications [3]. The paradigm of heterogeneous networks (HetNets) [4], composed of a hierarchy of macro cells enhanced by small cells of different sizes, has attracted lots of attention from both industry and academia. Macro cells with high-power base stations (BSs) provide ubiquitous coverage and small cells use various radio access technologies to serve user equipment terminals (UEs) with high data-rate demands. Unfortunately, the inter- and intra-tier interferences, resulting from densification of small cells, restrict the improvement of performance gains and commercial applications of HetNets.

At the same time, cloud computing has emerged as a popular computing paradigm for enhancing both spectral and energy efficiencies [5]. As an application of cloud computing to radio access networks, cloud radio access networks (C-RANs) have been proposed to achieve cooperative gains. In C-RANs, radio frequency processing is implemented at remote radio heads (RRHs) whereas baseband processing is centralized in a baseband unit (BBU) pool. However, the performance improvement of C-RANs is restricted by capacity-limited fronthaul links. Furthermore, since C-RANs are mainly used in hotspots to provide high data rates, control signalling and real-time voice service are not efficiently supported [6].

To overcome the aforementioned challenges, the concept of heterogeneous C-RANs (H-CRANs) was proposed in [7]. In H-CRANs, HetNets and C-RANs complement each other. Specifically, Macro BSs are connected to the BBU pool via backhaul with X2/S1 interfaces and RRHs are connected to the BBU pool through wired/wireless fronthaul. In addition to guaranteeing backward compatibility with existing cellular systems and providing ubiquitous connections, BSs are also responsible for delivering control signals and supporting low data-rate services. With the help of macro BSs, unnecessary handover and user re-association can be avoided. On the other hand, RRHs serve high data-rate applications in dedicated zones [8]. Besides, the data and control planes are decoupled and the delivery of control signals is shifted from RRHs to

macro BSs, thus the signalling overhead is reduced and the burden on fronthaul links is alleviated.

However, the constrained fronthaul capacity is still a bottleneck in H-CRANs, due to the large number of UEs and the increasing demands for high data-rate service in hotspots. Optical fiber links cannot be used violently because they are expensive. Wireless fronthaul is thought as an economic choice, but the spectrum resource is scarce. Therefore, a sharing strategy where fronthaul links share the spectrum resource with radio access networks has attracted lots of attention recently. Radio access network spectrum-based fronthauling has low sensitivity to propagation conditions, wider coverage, and the reusability of existing equipment. Many works, e.g., references [9–13], have investigated spectrum resource allocation between radio access networks and backhaul (fronthaul) links. References [9, 10] studied energy efficiency of HetNets with wireless backhaul, which accounted for the bandwidth and power allocated between macro cells, small cells, and backhaul. Reference [11] considered the joint design of transmit beamforming, power allocation, and spectrum splitting factors that took into account both uplink and downlink transmissions, then formulated a problem of maximizing the achievable sum-rate (SR). A joint problem of cell association and bandwidth allocation for wireless backhaul was optimized in [12]. Bandwidth allocation combined with interference mitigation techniques was optimized to maximize system SR using the large-dimensional random matrix theory in [13].

Besides, compressed-and-forward schemes are another effective way to deal with the challenge of limited fronthaul capacity [14, 15]. In the compressed-and-forward schemes, signals first are compressed at the BBU pool (or the RRHs) using point-to-point (P2P) compression or Wyner-Ziv (WZ) coding and then transmitted to the RRHs (or the BBU pool) in downlink (or uplink) via fronthaul. Therefore, the communication rates between the BBU pool and RRHs are reduced. Many works, such as references [16–19], have studied fronthaul compression for the uplink C-RAN. In [16], a weighted SR was maximized via the optimization of compression noise. In [17], the authors jointly designed fronthaul compression and beamforming to maximize the achievable SR in the uplink C-RAN with multi-antenna RRHs. An optimization problem was formulated in [18], where the compression and BS selection were performed jointly by introducing a sparsity-inducing term into the objective function. For the downlink C-RAN, the authors in [20, 21] studied the joint design of precoding and backhaul compression to maximize the system SR. Besides, a brief overview of fronthaul compression for both uplink and downlink was presented in [15, 22]. However, most of these works assumed that the fronthaul was composed of fiber links

with high cost and there was no consideration of spectrum resource sharing between radio access networks and fronthaul links. Moreover, these works were performed according to small-scale fading which varies in the order of milliseconds, thus resulting in much communication overhead for collecting channel information and high computational complexity to perform optimization in each coherence time of wireless channels.

Motivated by these facts, we aim to maximize the achievable ergodic SR of uplink H-CRANs with less complexity, overhead, and cost. This goal is also in line with the expectations of operators. One possible solution is to design the spectrum sharing strategy and compression noise simultaneously. This paper focuses on the uplink transmission of a H-CRAN, where many RRHs are embedded into a macro cell with a multiple-antenna BS. For economic reasons, only the BS are connected to the BBU pool via optical fiber links whereas the RRHs are connected to the BBU pool through wireless fronthaul links. Furthermore, the spectrum resource is shared between the radio access network and fronthaul links. Because the capacity of fronthaul links is limited, a two-stage compress-and-forward scheme is adopted. At the BBU side, the quantization bits are decompressed, followed by user message decoding. The contributions of this study are listed as follows.

- In this work, the spectrum sharing strategy and the compress-and-forward scheme are considered together to deal with the challenge of constrained fronthaul capacity. We formulate a joint optimization problem of bandwidth allocation and compression noise to maximize the achievable ergodic SR, which is a mixed time-scale issue. Because the bandwidth allocation is executed in a large time span whereas the compression noise design is performed in each small time span due to the dependence on small-scale fading. Besides, we consider not only different compress-and-forward schemes, i.e., P2P compression and WZ coding, but also different decoding strategies, i.e., the linear receptions with and without successive interference cancellation (SIC). These different compress-and-forward schemes and decoding strategies have a tradeoff between performance and complexity.
- In contrast to existing works [16, 17, 20, 21] where the SR maximization problems were based on fast-changing small-scale fading, we derive the deterministic approximation for the ergodic SR using large-dimensional random matrix theory. Then, an approximate problem of the original problem is introduced, which is a slow time-scale issue and only depends on statistical channel information. Therefore, the approximate problem can be solved with

less communication overhead for obtaining channel information and lower computational complexity.

- On the basis of deterministic expressions, we first give solutions to the two sub-problems of the joint optimization problem, then propose an algorithm based on Dinkelbach's algorithm to find the optimal solution to the approximation problem under different compression schemes and decoding strategies. Furthermore, we also propose a low-complexity algorithm to find the near optimal solution to the case of high signal-to-quantization-noise ratio (SQNR).

The remainder of this paper is organized as follows. In Section II, we describe the system model and formulate the optimization problem. Then the deterministic approximation of the ergodic SR is given in Section III. Based on the asymptotic result, we propose the algorithms to find solutions under different decoding schemes in Sections IV and V, followed by the analysis in special cases in Section VI. In Section VII, simulation results are presented and discussed. Finally, conclusion is drawn in Section VIII.

Notations: The notations are given as follows. Matrices and vectors are denoted by bold capital and lowercase symbols. $(\mathbf{A})^T$, $(\mathbf{A})^H$, and $\text{tr}(\mathbf{A})$ stand for transpose, conjugate transpose, and trace of \mathbf{A} , respectively. $\mathbf{A} \succeq \mathbf{0}$ ($\mathbf{A} \succ \mathbf{0}$) indicates that \mathbf{A} is a Hermitian positive semidefinite (definite) matrix. For a matrix $\mathbf{A} = [\mathbf{a}_1, \dots, \mathbf{a}_K] \in \mathbb{C}^{N \times K}$, $\mathbf{A}_{[m]} = [\mathbf{a}_1, \dots, \mathbf{a}_{m-1}, \mathbf{a}_{m+1}, \dots, \mathbf{a}_K] \in \mathbb{C}^{N \times K-1}$. The notations $\mathbb{E}(\cdot)$ and $\|\cdot\|$ are expectation and Euclidean norm operators, respectively. Finally, $\mathbf{a} \sim \mathcal{CN}(\mathbf{0}, \Sigma)$ is a complex Gaussian vector with zero-mean and covariance matrix Σ .

II. SYSTEM MODEL

As shown in Fig. 1, an uplink two-tier H-CRAN is considered, consisting of one N -antenna macro BS, L single-antenna RRHs, and one BBU pool. The BS is connected to the BBU pool using control and data interfaces, denoted as X2 and S1, via optical fiber links. The RRHs are connected to the BBU pool through noiseless wireless fronthaul links of capacity C_i in bps, $i = 1, 2, \dots, L$, which meet the constraint $\sum_{i=1}^L C_i \leq C$ [16]. Such a constraint can model the scenario where the RRHs access to the BBU pool via frequency/time division access scheme, and the number of access slots (frequency or time slots) shared among the RRHs is fixed and limited. The BS, acting as a centre controller, supports seamless coverage and provides service for K macro UEs (MUEs). The RRHs cooperate with each other and serve as hotspots for J small-cell

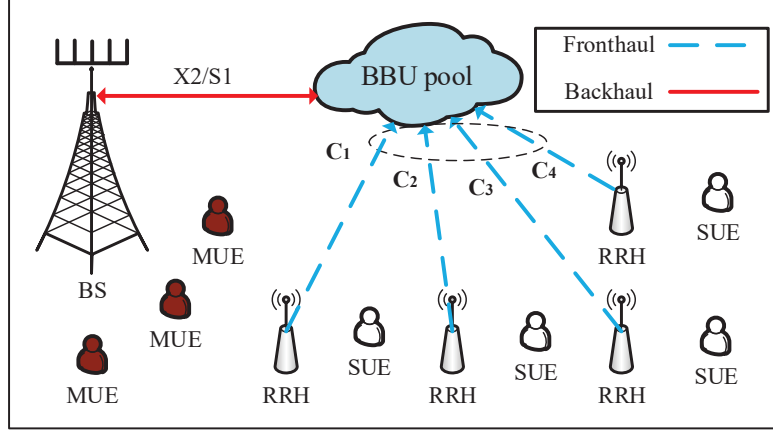


Fig. 1. System architecture of a H-CRAN.

UEs (SUEs). The MUEs and SUEs each have a single antenna and they simultaneously send messages to BSs and RRHs, respectively. We assume the messages sent from the MUEs can be received by both the BS and RRHs but SUEs' messages cannot be received by the BS directly (e.g., these SUEs are within far areas from the BS or shadow areas of buildings). SUEs' messages are transmitted to the BBU pool via the RRHs for processing and MUEs' messages are processed at the BS and BBU pool simultaneously. Finally, the processed signals are forwarded to the core network through the BS. Furthermore, owing to the limited fronthaul capacity, we assume a compress-and-forward scheme is implemented at these RRHs. More specifically, the RRHs first compress the received messages from the UEs and then transmit the quantized description toward the BBU pool. The BBU processor first decompresses the compressed version and then decodes the UEs' messages.

In the frequency domain, the dynamic allocation of bandwidth resource for wireless fronthaul and user communication is adopted. We assume that all the available bandwidth for the whole network is F Hz, which can be divided into two orthogonal parts $F_1 = \eta F$ and $F_2 = F - F_1$, such that $\eta \in [0, 1]$. The former is employed by the BS and RRHs to serve the MUEs and SUEs and the latter is dedicated to fronthaul links. It's assumed that $C = C_0 F_2$ where C_0 in bps/Hz is constant and depends on the specific propagation environment. Without losing generality, we normalize the fronthaul capacity constraint as $\sum_{i=1}^L \bar{C}_i \leq (1 - \eta) C_0$ where $\bar{C}_i = C_i / F$ in bps/Hz.

A. Achievable SR at BS

As discussed above, we assume the messages transmitted from the SUEs are only received at the RRHs while ones from the MUEs can be detected at both the BS and RRHs. Since we are concerned about the achievable SR of the MUEs and SUEs, we simply divide the achievable SR into two parts: one at the BS and the other at the central BBU pool. We first focus on the achievable SR at the BS.

The received signal $\mathbf{y}^{(B)} \in \mathbb{C}^{N \times 1}$ at the BS from the MUEs through sub-frequency band F_1 is expressed as

$$\mathbf{y}^{(B)} = \mathbf{H}\mathbf{x}^{(M)} + \mathbf{n}^{(B)}, \quad (1)$$

where $\mathbf{H} = [\mathbf{h}_1, \dots, \mathbf{h}_K] \in \mathbb{C}^{N \times K}$ is the channel matrix between the MUEs and BS, $\mathbf{h}_k = \sqrt{N\nu_k}\tilde{\mathbf{h}}_k$, $\tilde{\mathbf{h}}_k \sim \mathcal{CN}(\mathbf{0}, \frac{1}{N}\mathbf{I}_N)$ and ν_k represent the small-scale and large-scale fading coefficients, respectively [23], $\mathbf{n}^{(B)} \sim \mathcal{CN}(\mathbf{0}, \sigma^2\mathbf{I}_N)$ describes the independent additive white Gaussian noise (AWGN) [24], $\mathbf{x}^{(M)} = [x_1^{(M)}, \dots, x_K^{(M)}]^T \in \mathbb{C}^{K \times 1}$ is the signal vector of the MUEs with $x_k^{(M)} = \sqrt{p_k^{(M)}}s_k^{(M)}$, $s_k^{(M)} \sim \mathcal{CN}(0, 1)$ denotes the transmitted symbols of MUE k , and $p_k^{(M)}$ is the transmit power of MUE k .

Under the linear reception, the achievable ergodic SR of the MUEs at the BS in bps/Hz is computed as

$$R^{(B,L)}(\eta) = \eta R_0^{(B,L)} = \eta \sum_{k=1}^K R_{0,k}^{(B,L)}, \quad (2)$$

where

$$R_{0,k}^{(B,L)} = \mathbb{E} \left(\log_2 \frac{|\mathbf{H}\mathbf{P}^{(M)}\mathbf{H}^H + \sigma^2\mathbf{I}_N|}{|\mathbf{H}_{[k]}\mathbf{P}_{[k]}^{(M)}\mathbf{H}_{[k]}^H + \sigma^2\mathbf{I}_N|} \right), \quad (3)$$

in which $\mathbf{P}^{(M)} = \text{diag}(\mathbf{p}^{(M)})$ with $\mathbf{p}^{(M)} = [p_1^{(M)}, \dots, p_K^{(M)}]^T$. Note that the symbol “L” in the superscript suggests the linear reception. However, if the SIC method is applied, without losing generality, the decoding order is assumed as $1, 2, \dots, K$. Then the achievable SR at the BS becomes [22]

$$R^{(B,SIC)}(\eta) = \eta R_0^{(B,SIC)} = \eta \mathbb{E} \left(\sum_{k=1}^K \log_2 \frac{|\sum_{k'=k}^K p_{k'}^{(M)} \mathbf{h}_{k'} \mathbf{h}_{k'}^H + \sigma^2 \mathbf{I}_N|}{|\sum_{k'=k+1}^K p_{k'}^{(M)} \mathbf{h}_{k'} \mathbf{h}_{k'}^H + \sigma^2 \mathbf{I}_N|} \right), \quad (4)$$

$$= \eta \mathbb{E} \left(\log_2 \frac{|\mathbf{H}\mathbf{P}^{(M)}\mathbf{H}^H + \sigma^2 \mathbf{I}_N|}{|\sigma^2 \mathbf{I}_N|} \right). \quad (5)$$

Obviously, the achievable SR under the linear reception with SIC is greater than that under the linear reception without SIC due to less interference. But this advantage comes at the cost of higher computational complexity introduced by the SIC operation.

B. Achievable SR at BBU Pool

The received signals at the BBU pool includes those from both the SUEs and MUEs. To the RRHs, the MUEs and SUEs are equivalent. Therefore, for ease of expression, we define $\mathbf{G} = [\mathbf{G}^{(S)}, \mathbf{G}^{(M)}] \in \mathbb{C}^{L \times (J+K)}$ as a composite channel matrix, where $\mathbf{G}^{(S)}$ and $\mathbf{G}^{(M)}$ represent the channel matrix between the SUEs and RRHs and that between the MUEs and RRHs, respectively. $\mathbf{G}^{(S)} = [\mathbf{g}_1^{(S)}, \dots, \mathbf{g}_J^{(S)}]$, where $\mathbf{g}_j^{(S)} = [g_{j1}^{(S)}, \dots, g_{jL}^{(S)}]^T$, $g_{jl}^{(S)} = \sqrt{L\mu_{jl}^{(S)}}\tilde{g}_{jl}^{(S)}$ represents the channel coefficient between the j -th SUE and the l -th RRH, and $\mu_{jl}^{(S)}$ and $\tilde{g}_{jl}^{(S)} \sim \mathcal{CN}(0, \frac{1}{L})$ describe the corresponding large-scale and small-scale fading coefficients, respectively. $\mathbf{G}^{(M)}$ is similar to the definition of $\mathbf{G}^{(S)}$. We further define $\mathbf{x} = [(\mathbf{x}^{(S)})^T, (\mathbf{x}^{(M)})^T]^T$ as a composite signal vector, where $\mathbf{x}^{(S)}$ and $\mathbf{x}^{(M)}$ are the signal vectors from the SUEs and MUEs, respectively. $\mathbf{x}^{(S)} = [x_1^{(S)}, \dots, x_J^{(S)}]^T$, where $x_j^{(S)} = \sqrt{p_j^{(S)}}s_j^{(S)}$, $s_j^{(S)} \sim \mathcal{CN}(0, 1)$ is the signal transmitted by SUE j , and $p_j^{(S)}$ denotes the transmit power of SUE j . Thus the received signal at RRH l is expressed as

$$y_l^{(R)} = \sum_{m=1}^M g_{lm}x_m + n_l^{(R)}, \quad (6)$$

where $M = J + K$, $n_l^{(R)} \sim \mathcal{CN}(0, \sigma^2)$ represents the AWGN at AP l , x_m denotes the m -th element of \mathbf{x} , and g_{lm} is the (l, m) -th element of \mathbf{G} .

We assume the compress-and-forward scheme is applied at the RRHs, e.g., point-to-point (P2P) compression [25] or Wyner-Ziv (WZ) coding [16]. The RRHs first quantizes the received signal $\mathbf{y}^{(R)} = [y_1^{(R)}, \dots, y_L^{(R)}]^T$ into $\tilde{\mathbf{y}}^{(\kappa)} = [\tilde{y}_1^{(\kappa)}, \dots, \tilde{y}_L^{(\kappa)}]^T$ (the superscript “ κ ” can be P2P or WZ indicating different quantization schemes adopted), and then transmits the compressed version to the BBU pool for central processing through wireless fronthaul links. At the BBU side, the quantization codewords are decompressed and then the messages are decoded [17]. In this work, we obtain the achievable rate region in the case where each RRH only compresses its own received signal. Similar to reference [15], we model the relationship between the received signal $y_l^{(R)}$ and its compressed description $\tilde{y}_l^{(\kappa)}$ as Gaussian test channel,

$$\tilde{y}_l^{(\kappa)} = y_l^{(R)} + q_l, \quad (7)$$

where $q_l \sim \mathcal{CN}(0, \psi_l^2)$ is independent quantization noise and ψ_l^2 describes the variance of the quantization noise at RRH l .

In the case of the linear reception at the BBU pool, the achievable ergodic SR is

$$R^{(P,L)}(\eta, \Psi) = \eta R_0^{(P,L)}(\Psi) = \eta \sum_{m=1}^M R_{0,m}^{(P,L)}(\Psi), \quad (8)$$

where

$$R_{0,m}^{(P,L)}(\Psi) = \mathbb{E} \left(\log_2 \frac{|\mathbf{G}\mathbf{P}\mathbf{G}^H + \Psi + \sigma^2\mathbf{I}_L|}{|\mathbf{G}_{[m]}\mathbf{P}_{[m]}\mathbf{G}_{[m]}^H + \Psi + \sigma^2\mathbf{I}_L|} \right), \quad (9)$$

in which Ψ is an $L \times L$ diagonal matrix with diagonal elements $\{\psi_l^2\}$'s, $\mathbf{P} = \text{diag}(\mathbf{p})$ with $\mathbf{p} = [(\mathbf{p}^{(S)})^T, (\mathbf{p}^{(M)})^T]^T$, and $\mathbf{p}^{(S)} = [p_1^{(S)}, \dots, p_J^{(S)}]^T$.

When the SIC method is employed, without loss of generality, the decoding order is assumed as $1, 2, \dots, M$ [26–28]. Then the achievable ergodic SR of the SUEs and MUEs at the BBU is expressed as

$$R^{(P,SIC)}(\eta, \Psi) = \eta R_0^{(P,SIC)}(\Psi) = \eta \mathbb{E} \left(\sum_{m=1}^M \log_2 \frac{|\sum_{m'=m}^M p_{m'} \mathbf{g}_{m'} \mathbf{g}_{m'}^H + \Psi + \sigma^2 \mathbf{I}_L|}{|\sum_{m'=m+1}^M p_{m'} \mathbf{g}_{m'} \mathbf{g}_{m'}^H + \Psi + \sigma^2 \mathbf{I}_L|} \right), \quad (10)$$

$$= \eta \mathbb{E} \left(\log_2 \frac{|\mathbf{G}\mathbf{P}\mathbf{G}^H + \Psi + \sigma^2 \mathbf{I}_L|}{|\Psi + \sigma^2 \mathbf{I}_L|} \right). \quad (11)$$

In what follows we give the fronthaul constraints that must be satisfied to achieve the SRs in (11) and (8) under two different compression strategies, i.e., P2P compression and WZ coding, respectively.

1) P2P Compression Scheme: As a consequence of P2P compression, each RRH produces a binary string that allows the decompressor unit at the BS to identify the quantized signal from a certain codebook in parallel [15]. According to rate-distortion theory, the signal $\tilde{y}^{(P2P)}$ can be recovered if the fronthaul rate satisfies the condition

$$R^{(fh,P2P)}(\eta, \Psi) = \eta R_0^{(fh,P2P)}(\Psi) = \eta \mathbb{E} \left(\sum_{l=1}^L \log_2 \frac{\sum_{m=1}^M p_m |g_{lm}|^2 + \sigma^2 + \psi_l^2}{\psi_l^2} \right) \leq (1 - \eta) C_0. \quad (12)$$

This constraint suggests that, from an intuitive level, larger ψ_l^2 's cause a smaller $R_0^{(fh,P2P)}(\eta, \Psi)$ and thus less bandwidth is required by fronthaul. However, such separate and independent processing does not take into account the statistical correlation across the signals $y_l^{(R)}$, $l = 1, \dots, L$, received at different RRHs [22], which can be used as side information when the BBU

decompresses the quantized signals from the RRHs. WZ coding provides an efficient way to leverage the side information available at the RRHs.

2) *WZ Coding Scheme*: Taking advantage of the correlation of the received signals at all the RRHs which results from the mutual interference between UEs, WZ coding can achieve a higher performance and make better use of limited fronthaul capacity than P2P compression [15]. WZ coding enables the compressor to use a finer quantizer and associate the same binary string to a subset of codewords, whereas P2P compression associates a distinct binary string with each codeword in the quantization codebook. According to **Proposition 1** in [16], the SRs in (11) and (8) can be achieved if the condition

$$R^{(fh,WZ)}(\eta, \Psi) = \eta R_0^{(fh,WZ)}(\Psi) = \eta E \left(\log_2 \frac{|\mathbf{G}\mathbf{P}\mathbf{G}^H + \Psi + \sigma^2 \mathbf{I}_L|}{|\Psi|} \right) \leq (1 - \eta)C_0, \quad (13)$$

is satisfied.

C. Problem Formulation

By jointly designing the compression noise variance matrix Ψ and the bandwidth allocation factor η , the achievable ergodic SR maximization problem can be formulated as:

$$\max_{\eta, \Psi} R^{(B,\zeta)}(\eta, \Psi) + R^{(P,\zeta)}(\eta, \Psi) \quad (14a)$$

$$\text{s.t. } R^{(fh,\kappa)}(\eta, \Psi) \leq (1 - \eta)C_0, \quad (14b)$$

$$\eta \in [0, 1], \quad (14c)$$

$$\Psi_{ll} \geq 0, \quad l = 1, 2, \dots, L, \quad (14d)$$

$$\Psi_{l'l} = 0, \quad l' \neq l, \quad (14e)$$

where the symbol “ ζ ” in the superscript can be “L” or “SIC” representing different decoding strategies (i.e., the linear receptions with and without SIC), the fronthaul constraint (14b) can be either (12) or (13), depending on the specific compression strategy. Constraints (14d) and (14e) indicate that Ψ is a diagonal matrix. The objective function is a difference-of-convex problem and some algorithms are proposed in [16, 20, 29] to solve related problems. However, since the optimization of (η, Ψ) is based on the ergodic SR, Monte Carlo averaging over channels needs a lot of samples to capture the variations of both large-scale fading and small-scale fading. Because small-scale fading varies at the level of milliseconds, collecting channel information leads to too

much communication overhead and calculating average results over channels also brings more prohibitively computational complexity. Besides, the bandwidth allocation problem is a slow time-scale issue because it is usually executed in a large time span whereas the compression noise design problem is a fast time-scale issue since it is performed in each small time span (for example, a coherence time interval of wireless channels) due to its dependence on fast-changing small-scale fading. Therefore, the joint problem is a mixed time-scale issue. To address these challenges, we first introduce the asymptotic expression of the ergodic SR in the large-system regime and then find solutions based on the deterministic approximation in the following sections.

III. DETERMINISTIC EQUIVALENTS

In the following, we understand the ergodic SR in the large-system regime [30, 31] where K , J , N , and L grow infinitely while keeping fixed ratios $\chi_1 = K/N$ and $\chi_2 = M/L$ such that $0 < \liminf_N \chi_1 < \limsup_N \chi_1 < 1$ and $0 < \liminf_L \chi_2 < \limsup_L \chi_2 < 1$ [13]. For notational convenience, we use $N \rightarrow \infty$ and $L \rightarrow \infty$ to refer to $N, K \rightarrow \infty$ and $L, M \rightarrow \infty$, respectively. We will derive deterministic approximations $\bar{R}^{(B,\varsigma)}(\eta)$, $\bar{R}^{(P,\varsigma)}(\eta, \Psi)$, and $\bar{R}^{(fh,\kappa)}(\eta, \Psi)$ of the ergodic SRs $R^{(B,\varsigma)}(\eta)$, $R^{(P,\varsigma)}(\eta, \Psi)$, and $R^{(fh,\kappa)}(\eta, \Psi)$, respectively.

A. Deterministic Equivalents for $R^{(B,SIC)}(\eta)$ and $R^{(B,L)}(\eta)$

Since $\tilde{\mathbf{h}}_k$'s are independently and identically distributed (i.i.d.) complex Gaussian variables whose real and imaginary parts are independent. According to references [32, 33], we have the following lemma.

Lemma 1. *Given that $\tilde{\mathbf{h}}_k$'s are i.i.d. complex Gaussian variables with independent real and imaginary parts, as $N \rightarrow \infty$, we have $R^{(B,SIC)}(\eta) - \bar{R}^{(B,SIC)}(\eta) \rightarrow 0$, where $\bar{R}^{(B,SIC)}(\eta) = \eta \bar{R}_0^{(B,SIC)}$ and*

$$\bar{R}_0^{(B,SIC)} = \frac{1}{\log 2} (\Delta_0 - \log |\sigma^2 \mathbf{I}_N|), \quad (15)$$

where

$$\Delta_0 = \log |\mathbf{\Gamma}| + \sum_{k=1}^K \left(\frac{1}{1 + e_k} - \log \frac{1}{1 + e_k} \right) - K, \quad (16)$$

in which $e_k = p_k^{(M)} \nu_k \text{tr}(\mathbf{\Gamma}^{-1})$ and

$$\mathbf{\Gamma} = \left(\sum_{k=1}^K \frac{p_k^{(M)} \nu_k}{1 + e_k} + \sigma^2 \right) \mathbf{I}_N. \quad (17)$$

In the case of the linear reception without SIC, as $N \rightarrow \infty$, the deterministic equivalent of $R^{(B,L)}$ is given as $R^{(B,L)}(\eta) - \bar{R}^{(B,L)}(\eta) \rightarrow 0$, where $\bar{R}^{(B,L)}(\eta) = \eta \bar{R}_0^{(B,L)} = \eta \sum_{k=1}^K \bar{R}_{0,k}^{(B,L)}$ and $\bar{R}_{0,k}^{(B,L)} = \frac{1}{\log 2} (\Delta_0 - \Delta_k)$ in which

$$\Delta_k = \log |\tilde{\mathbf{\Gamma}}_k| + \sum_{k'=1, k' \neq k}^K \left(\frac{1}{1 + \tilde{e}_{kk'}} - \log \frac{1}{1 + \tilde{e}_{kk'}} \right) - (K - 1), \quad (18)$$

with $\tilde{e}_{kk'} = p_{k'}^{(M)} \nu_{k'} \text{tr} \tilde{\mathbf{\Gamma}}_k^{-1}$ and

$$\tilde{\mathbf{\Gamma}}_k = \left(\sum_{k'=1, k' \neq k}^K \frac{p_{k'}^{(M)} \nu_{k'}}{1 + \tilde{e}_{kk'}} + \sigma^2 \right) \mathbf{I}_N. \quad (19)$$

Proof: Refer to Appendix A.

B. Deterministic Equivalents for $R^{(P,SIC)}(\eta, \Psi)$ and $R^{(P,L)}(\eta, \Psi)$

Based on the analysis of $\bar{R}^{(B,\varsigma)}(\eta)$ in Section III-A, we use large-dimensional random matrix theory again to derive the deterministic equivalents of $R^{(P,SIC)}(\eta, \Psi)$ and $R^{(P,L)}(\eta, \Psi)$ in the following lemma.

Lemma 2. Given that $\tilde{\mathbf{g}}_m$'s are i.i.d. complex Gaussian variables with independent real and imaginary parts, as $L \rightarrow \infty$, we have $R^{(P,SIC)}(\eta, \Psi) - \bar{R}^{(P,SIC)}(\eta, \Psi) \rightarrow 0$, where $\bar{R}^{(P,SIC)}(\eta, \Psi) = \eta \bar{R}_0^{(P,SIC)}(\Psi)$ and

$$\bar{R}_0^{(P,SIC)}(\Psi) = \frac{1}{\log 2} (\nabla_0 - \log |\Psi + \sigma^2 \mathbf{I}_L|), \quad (20)$$

where

$$\nabla_0 = \log |\mathbf{\Lambda}| + \sum_{m=1}^M \left(\frac{1}{1 + b_m} - \log \frac{1}{1 + b_m} \right) - M, \quad (21)$$

in which $b_m = p_m \text{tr} (\mathbf{U}_m \mathbf{\Lambda}^{-1})$ and

$$\mathbf{\Lambda} = \sum_{m=1}^M \frac{p_m \mathbf{U}_m}{1 + b_m} + \Psi + \sigma^2 \mathbf{I}_L, \quad (22)$$

with $\mathbf{U}_m = \text{diag}(\mathbf{u}_m)$ and $\mathbf{u}_m = [\mu_{1m}, \dots, \mu_{Lm}]^T$.

In the case of the linear reception without SIC, we have $R^{(P,L)}(\eta, \Psi) - \bar{R}^{(P,L)}(\eta, \Psi) \rightarrow 0$, where $\bar{R}^{(P,L)}(\eta, \Psi) = \eta \bar{R}_0^{(P,L)}(\Psi) = \eta \sum_{m=1}^M \bar{R}_{0,m}^{(P,L)}(\Psi)$ and $\bar{R}_{0,m}^{(P,L)}(\Psi) = \frac{1}{\log 2}(\nabla_0 - \nabla_m)$ in which

$$\nabla_m = \log |\tilde{\Lambda}_m| + \sum_{m'=1, m' \neq m}^M \left(\frac{1}{1 + b_{mm'}} - \log \frac{1}{1 + b_{mm'}} \right) - (M - 1), \quad (23)$$

with $\tilde{b}_{mm'} = p_{m'} \text{tr} \left(\mathbf{U}_{m'} \tilde{\Lambda}_m^{-1} \right)$ and

$$\tilde{\Lambda}_m = \sum_{m'=1, m' \neq m}^M \frac{p_{m'} \mathbf{U}_{m'}}{1 + \tilde{b}_{mm'}} + \Psi + \sigma^2 \mathbf{I}_L. \quad (24)$$

Proof: Refer to the proof of $\bar{R}^{(B,\varsigma)}(\eta)$ in Appendix A, due to the similarity between $R^{(B,\varsigma)}(\eta)$ and $R^{(P,\varsigma)}(\eta, \Psi)$.

C. Deterministic Equivalents for $R^{(fh,WZ)}(\eta, \Psi)$ and $R^{(fh,P2P)}(\eta, \Psi)$

Then, we also give two deterministic equivalents of fronthaul constraints $R^{(fh,P2P)}(\eta, \Psi)$ and $R^{(fh,WZ)}(\eta, \Psi)$ for two different compression strategies, i.e., P2P compression and WZ coding.

1) *P2P compression:* Observe that if M is large enough, according to the law of large numbers, $\sum_{m=1}^M p_m |g_{lm}|^2$ converges to its mean,

$$\frac{1}{M} \sum_{m=1}^M p_m |g_{lm}|^2 \xrightarrow{M \rightarrow \infty} \frac{1}{M} \sum_{m=1}^M p_m \mu_{lm}, \quad (25)$$

where μ_{lm} is the large-scale fading coefficient between RRH l and UE m . Therefore, the deterministic approximation of $R^{(fh,P2P)}(\eta, \Psi)$ in (12) is given by the following lemma.

Lemma 3. According to the law of large numbers, we have the result in (25) and $R^{(fh,P2P)}(\eta, \Psi) - \bar{R}^{(fh,P2P)}(\eta, \Psi) \xrightarrow{M \rightarrow \infty} 0$, where $\bar{R}^{(fh,P2P)}(\eta, \Psi) = \eta \bar{R}_0^{(fh,P2P)}(\Psi)$ and

$$\bar{R}_0^{(fh,P2P)}(\Psi) = \sum_{l=1}^L \log_2 \frac{\sum_{m=1}^M p_m \mu_{lm} + \sigma^2 + \psi_l^2}{\psi_l^2}. \quad (26)$$

2) *WZ compression:* Due to the similarity of $R^{(P,SIC)}(\eta, \Psi)$ and $R^{(fh,WZ)}(\eta, \Psi)$, we directly give the deterministic equivalent of $R^{(fh,WZ)}(\eta, \Psi)$ as the following lemma according to **Lemma 2**.

Lemma 4. *Given that $\tilde{\mathbf{g}}_m$'s are i.i.d. complex Gaussian variables with independent real and imaginary parts, as $L \rightarrow \infty$, we have $R^{(fh,WZ)}(\eta, \Psi) - \bar{R}^{(fh,WZ)}(\eta, \Psi) \rightarrow 0$, where $\bar{R}^{(fh,WZ)}(\eta, \Psi) = \eta \bar{R}_0^{(fh,WZ)}(\Psi)$ and*

$$\bar{R}_0^{(fh,WZ)}(\Psi) = \frac{1}{\log 2} (\nabla_0 - \log |\Psi|), \quad (27)$$

in which ∇_0 is given in (21).

Note that one thing these approximations have in common is that they are determined by statistical channel knowledge (i.e., large-scale fading), instead of small-scale fading. Generally, statistical channel knowledge varies much slower than small-scale fading. Thus the communication overhead for obtaining channel information is reduced significantly.

IV. JOINT DESIGN UNDER LINEAR RECEPTION WITH SIC

Problem (14) has different forms because different decoding strategies and compression schemes are included simultaneously. For analytical ease, problem (14) is separated into two problems according to decoding strategies and we first consider the case of the linear reception with SIC. By replacing $R^{(B,SIC)}(\eta)$, $R^{(P,SIC)}(\eta, \Psi)$, and $R^{(fh,\kappa)}(\eta, \Psi)$ with their deterministic equivalents $\bar{R}^{(B,SIC)}(\eta)$, $\bar{R}^{(P,SIC)}(\eta, \Psi)$, and $\bar{R}^{(fh,\kappa)}(\eta, \Psi)$, respectively, we introduce an alternative to problem (14) as follows:

$$\max_{\eta, \Psi} \quad \bar{R}^{(B,SIC)}(\eta, \Psi) + \bar{R}^{(P,SIC)}(\eta, \Psi) \quad (28a)$$

$$\text{s.t.} \quad \bar{R}^{(fh,\kappa)}(\eta, \Psi) \leq (1 - \eta)C_0, \quad (28b)$$

$$(14c) - (14e), \quad (28c)$$

which avoids redundant computation resulting from Monte Carlo averaging over channels, because the objective function and fronthaul constraint are only dependent on statistical channel knowledge and irrelevant to small-scale fading. Furthermore, the joint optimization problem (14) of the bandwidth allocation and compression noise design now turns into a slow time-scale issue and we can find solutions to the joint optimization problem (28) in a large time span, not each small time span. However, finding the global optimal results of problem (28) is still a challenge due to the non-convexity of the objective function over variable matrix Ψ . In what follows, we first analyze two sub-problems of problem (28): 1) find the optimal Ψ given that η is fixed, and

2) find the optimal η given that Ψ is fixed. Then we reformulate problem (28) as a concave-convex fractional programming [34, 35]. Finally, an algorithm is proposed to find solutions to the joint optimization problem of Ψ and η .

A. Optimization of Fronthaul Compression

Given a fixed η value, We find the optimal value of Ψ by solving the following sub-problem:

$$\max_{\Psi} \quad \bar{R}^{(P,SIC)}(\Psi) \quad (29a)$$

$$\text{s.t.} \quad (28b), (14d), \text{ and } (14e), \quad (29b)$$

which is still non-convex because the objective function $\bar{R}^{(P,SIC)}(\Psi)$ is actually a convex function, instead of a concave function, with respect to Ψ . Thanks to the following lemma, which sheds light on solving problem (29).

Lemma 5 ([36]). *Given an $L \times L$ complex matrix $\Gamma \succ \mathbf{0}$. Consider the function $f(\Omega) = -\text{tr}(\Omega\Gamma) + \log |\Omega| + L$, then*

$$\log |\Gamma^{-1}| = \max_{\Omega \in \mathbb{C}^{L \times L}, \Omega \succeq \mathbf{0}} f(\Omega), \quad (30)$$

with the optimal solution $\Omega^* = \Gamma^{-1}$.

From **Lemma 5**, the inequality

$$-\log |\Gamma| \geq \log |\Omega| - \text{tr}(\Omega\Gamma) + L, \quad (31)$$

always holds and the equality holds with $\Omega = \Gamma^{-1}$. By applying inequality (31) to the second term of $\bar{R}^{(P,SIC)}(\Psi)$ via setting $\Gamma = \Psi + \sigma^2 \mathbf{I}_L$, then we reformulate sub-problem (29) as

$$\max_{\Psi, \Omega} \quad \tilde{\bar{R}}^{(P,SIC)}(\Psi, \Omega) \quad (32a)$$

$$\text{s.t.} \quad (28b), (14d), \text{ and } (14e), \quad (32b)$$

where $\tilde{\bar{R}}^{(P,SIC)}(\Psi, \Omega) = \eta \bar{R}_0^{(P,SIC)}(\Psi, \Omega)$ and

$$\bar{R}_0^{(P,SIC)}(\Psi, \Omega) = \frac{1}{\log 2} \{ \nabla_0 + \log |\Omega| - \text{tr}[\Omega(\Psi + \sigma^2 \mathbf{I}_L)] + L \}. \quad (33)$$

Assume that Ψ^* is the optimal result. Now, for problem (32) the optimal value of Ω , according to **Lemma 5**, is

$$\Omega^* = (\Psi^* + \sigma^2 \mathbf{I}_L)^{-1}. \quad (34)$$

We observe that $\tilde{R}^{(P,SIC)}(\Psi, \Omega)$ is nonconvex over both Ψ and Ω . However, it is convex over either Ψ or Ω when the other one is fixed. Besides, the fronthaul constraint $\bar{R}^{(fh,\kappa)}(\Psi)$ is convex over Ψ , no matter what compression scheme is adopted. Therefore, an iterative coordinate ascent algorithm is proposed to find solutions to problem (32), as shown in **Algorithm 1**.

Note that the objective function of problem (32) is continuously differentiable and the feasible set is nonempty, closed, and convex. Furthermore, the iterates $(\Psi^{(t)}, \Omega^{(t)})$ of **Algorithm 1** are bounded due to the fronthaul capacity constraint. **Algorithm 1** yields a nondecreasing sequence of objective values for problem (32). According to [37, Corollary 2], it can be verified that **Algorithm 1** converges to a stationary point of problem (32). Given that (Ψ^*, Ω^*) is a stationary point of problem (32), then we have

$$\text{tr} \left(\nabla_{\Psi} \tilde{R}^{(P,SIC)}(\Psi^*, \Omega^*)^H (\Psi - \Psi^*) \right) \leq 0, \forall \Psi \in \mathcal{W}, \quad (35)$$

where $\mathcal{W} = \{\Psi | (28b), (14d), \text{ and } (14e)\}$ and $\nabla_{\Psi} \tilde{R}^{(P,SIC)}(\Psi^*, \Omega^*)$ denotes the gradient of $\tilde{R}^{(P,SIC)}(\Psi^*, \Omega^*)$ with respect to Ψ . Substituting $\Omega^* = (\Psi^* + \sigma^2 \mathbf{I}_L)^{-1}$ into (35), then it can be verified $\nabla_{\Psi} \tilde{R}^{(P,SIC)}(\Psi^*) = \nabla_{\Psi} \tilde{R}^{(P,SIC)}(\Psi^*, (\Psi^* + \sigma^2 \mathbf{I}_L)^{-1})$. Therefore, (Ψ^*, Ω^*) is also a stationary point of problem (29).

Algorithm 1 Optimal algorithm for problem (32).

Input: Large-scale channel coefficients and the tolerance factor ϵ .

Output: Ψ .

- 1: **Initialization:** $\Psi^{(0)} = \sigma^2 \mathbf{I}_L$, $\Omega^{(0)} = (\Psi^{(0)} + \sigma^2 \mathbf{I}_L)^{-1}$, and $t = 1$. Calculate $\tilde{R}^{(P,SIC,0)}$.
 - 2: Given $\Omega^{(t-1)}$, find the optimal $\Psi^{(t)}$ via solving problem (32).
 - 3: Update $\Omega^{(t)} = (\Psi^{(t)} + \sigma^2 \mathbf{I}_L)^{-1}$ and $\tilde{R}^{(P,SIC,t)}$.
 - 4: **if** $(|\tilde{R}^{(P,SIC,t)}(\Psi^{(t)}, \Omega^{(t)}) - \tilde{R}^{(P,SIC,t-1)}(\Psi^{(t-1)}, \Omega^{(t-1)})| > \epsilon)$ **then**
 - 5: $t = t + 1$ and go to Step 2;
 - 6: **else**
 - 7: **return** $\Psi^{(t)}$.
 - 8: **end if**
-

B. Optimization of Bandwidth Allocation

Once the optimal value of Ψ is obtained from problem (32), it can be used in the following optimization problem of bandwidth allocation:

$$\max_{\eta} \quad \bar{R}^{(B,SIC)}(\eta) + \bar{R}^{(P,SIC)}(\eta) \quad (36a)$$

$$\text{s.t.} \quad (28b) \quad \text{and} \quad (14c), \quad (36b)$$

which is a linear problem over η . Therefore, the optimal value of η is given as

$$\eta^* = \frac{C_0}{\bar{R}_0^{(fh,\kappa)} + C_0}. \quad (37)$$

Note that the bandwidth allocation factor η increases as the normalized fronthaul capacity C_0 rises, typically when $C_0 \rightarrow \infty$, $\eta \rightarrow 1$. That is to say, all bandwidth should be used in radio access networks if there is no limitation on fronthaul. However, as $C_0 \rightarrow 0$, suggesting that the unit fronthaul capacity is small, then more bandwidth should be allocated to fronthaul links when fronthaul compression noise is fixed.

C. Joint Optimization of Ψ and η

By substituting the optimal value of η given by (37) into (28a), we reformulate an equivalent problem of problem (28) as

$$\max_{\Psi} \quad \frac{\bar{R}_0^{(B,SIC)}(\Psi) + \bar{R}_0^{(P,SIC)}(\Psi)}{\bar{R}_0^{(fh,\kappa)}(\Psi) + C_0} \quad (38a)$$

$$\text{s.t.} \quad (14d) \quad \text{and} \quad (14e), \quad (38b)$$

which is a fractional programming whose numerator and denominator are both convex with respect to Ψ . For the convenience of designing the related algorithm, we apply the inequality (31) again to the numerator of (38a), thus problem (38) becomes

$$\max_{\Psi, \Omega} \quad \frac{f(\Psi, \Omega)}{g(\Psi)} \quad (39a)$$

$$\text{s.t.} \quad (14d) \quad \text{and} \quad (14e), \quad (39b)$$

where $f(\Psi, \Omega) = \bar{R}_0^{(B,SIC)} + \tilde{\bar{R}}_0^{(P,SIC)}(\Psi, \Omega)$ and $g(\Psi) = \bar{R}_0^{(fh,\kappa)}(\Psi) + C_0$. Therefore, the object function in (39a) is a concave-convex fractional function over Ψ but a concave function over Ω , respectively. Before the algorithm to find the optimal solutions is presented, we first define

the set $\mathcal{S} = \{\Psi | \Psi_{ll} \geq 0, \Psi_{ll'} = 0, l \neq l', l = 1, \dots, L\}$ to describe constraints (14d) and (14e) and introduce the following proposition:

Proposition 1. *Assume that $f(\Psi, \Omega)$ and $g(\Psi)$ are continuous, and $f(\Psi, \Omega)$ is positive. Given $\Psi^* \in \mathcal{S}$, $\Omega^* = (\Psi^* + \sigma^2 \mathbf{I}_L)^{-1}$, and $\omega^* = \frac{f(\Psi^*, \Omega^*)}{g(\Psi^*)}$. Then $\Psi^* \in \mathcal{S}$ is the optimal solution to problem (39) if and only if*

$$(\Psi^*, \Omega^*) = \arg \max_{\Psi \in \mathcal{S}, \Omega} [f(\Psi, \Omega) - \omega^* g(\Psi)]. \quad (40)$$

Proof: See Appendix B for reference.

Proposition 1 suggests that we can find the optimal solutions to fractional problem (39) by finding the unique zero of the auxiliary function $F(\omega) = f(\Psi, \Omega) - \omega g(\Psi)$. Therefore, we propose an algorithm based on Dinkelbach's algorithm [34, 35], as shown in **Algorithm 2**.

Algorithm 2 is a two-level iterative algorithm. The inner iteration aims to make $F(\omega)$ converge to a certain value with a given ω and the outer iteration tries to find a typical value ω^* which establishes the equality $F(\omega^*) = 0$.

The convergence of **Algorithm 2** is given by the following proposition.

Proposition 2. *Algorithm 2 converges to the solution of Proposition 1.*

Proof: Refer to Appendix C.

Since **Algorithm 2** translates the original concave-convex problem into a sequence of auxiliary subproblems indexed by the parameter ω , the overall computational complexity relies on the complexities of all subproblems and the convergence rate of the subproblem sequence. To explain the convergence of subproblem sequence, we rewritten (67) as

$$\omega^{(t+1)} = \omega^{(t)} - \frac{F(\omega^{(t)})}{F'(\omega^{(t)})}, \quad (41)$$

where $F'(\omega^{(t)}) = \frac{\partial F(\omega^{(t)})}{\partial \omega^{(t)}}$. Equation (41) can be interpreted as an application of Newton's method to $F(\omega)$ so that the subproblem sequence in **Algorithm 2** converges at a super-linear rate [35].

Algorithm 2 Joint optimization algorithm for problem (39).

Input: Large-scale channel coefficients and the tolerance factors ϵ_1 and ϵ_2 .

Output: Ψ .

```

1: Initialization:  $\underline{\Psi}^{(0)} = \sigma^2 \mathbf{I}_L$ ,  $\Omega^{(0)} = (\underline{\Psi}^{(0)} + \sigma^2 \mathbf{I}_L)^{-1}$ ,  $\omega^{(0)} = 0$ , and  $t = 0$ .
2: while  $F(\omega^{(t)}) > \epsilon_1$  do
3:    $G^{(0)} = f(\Psi^{(0)}, \Omega^{(0)}) - \omega^{(t)} g(\Psi^{(0)})$ .
4:    $i = 1$ ;
5:    $\underline{\Psi}^{(i)} = \arg \max_{\Psi \in \mathcal{S}} \{f(\Psi, \Omega^{(i-1)}) - \omega^{(t)} g(\Psi)\}$ .
6:   Update  $\Omega^{(i)} = (\underline{\Psi}^{(i)} + \sigma^2 \mathbf{I}_L)^{-1}$ .
7:    $G^{(i)} = f(\underline{\Psi}^{(i)}, \Omega^{(i)}) - \omega^{(t)} g(\underline{\Psi}^{(i)})$ .
8:   if  $|G^{(i)} - G^{(i-1)}| > \epsilon_2$  then
9:      $i = i + 1$  and go to Step 5;
10:  else
11:     $\Psi^{(t)} = \underline{\Psi}^{(i)}$ .
12:  end if
13:   $F(\omega^{(t)}) = f(\Psi^{(t)}, \Omega^{(t)}) - \omega^{(t)} g(\Psi^{(t)})$ .
14:   $\omega^{(t+1)} = \frac{f(\Psi^{(t)}, \Omega^{(t)})}{g(\Psi^{(t)})}$ .
15:   $t = t + 1$ .
16: end while
17: return  $\Psi^{(t-1)}$ .
```

V. JOINT DESIGN UNDER LINEAR RECEPTION WITHOUT SIC

In the case of the linear reception without SIC, the joint optimization problem is formulated as:

$$\max_{\eta, \Psi} \quad \bar{R}^{(B,L)}(\eta) + \bar{R}^{(P,L)}(\eta, \Psi) \quad (42a)$$

$$\text{s.t.} \quad (14c) - (14e) \text{ and } (28b). \quad (42b)$$

Similar to the analysis on problem (38) whose achievable SR is based on the linear reception with SIC, we translate problem (42) into a concave-convex fractional programming formulated

as:

$$\max_{\Psi, \{\Omega_m\}_{m=1}^M} \frac{\bar{R}_0^{(B,L)} + \tilde{\bar{R}}_0^{(P,L)}(\Psi, \{\Omega_m\}_{m=1}^M)}{\bar{R}_0^{(fh,\kappa)}(\Psi) + C_0} \quad (43a)$$

$$\text{s.t. (14d) and (14e),} \quad (43b)$$

where $\tilde{\bar{R}}_0^{(P,L)}(\Psi, \{\Omega_m\}_{m=1}^M) = \sum_{m=1}^M \tilde{\bar{R}}_{0,m}^{(P,L)}(\Psi, \Omega_m)$ and

$$\begin{aligned} \tilde{\bar{R}}_{0,m}^{(P,L)}(\Psi, \Omega_m) = & \frac{1}{\log 2} \left[\nabla_0 + \log |\Omega_m| - \text{tr}(\Omega_m \tilde{\Lambda}_m) + L \right. \\ & \left. - \sum_{m'=1, m' \neq m}^M \left(\frac{1}{1+b_{mm'}} - \log \frac{1}{1+b_{mm'}} \right) - (M-1) \right]. \end{aligned} \quad (44)$$

Actually, problem (43) can also be solved via **Algorithm 2** with some modification as follows:

- Replace auxiliary function $f(\Psi, \Omega)$ with a new defined auxiliary function

$$\bar{f}(\Psi, \{\Omega_m\}_{m=1}^M) = R_0^{(B,L)} + \sum_{m=1}^M \tilde{\bar{R}}_{0,m}^{(P,L)}(\Psi, \Omega_m).$$

- Update (initialize) $\Omega_m^{(i)} = \left(\sum_{m'=1, m' \neq m}^M \frac{p_{m'} \mathbf{U}_{m'}}{1+b_{mm'}} + \underline{\Psi}^{(i)} + \sigma^2 \mathbf{I}_L \right)^{-1}$, for $m = 1, \dots, M$.

VI. SUBOPTIMAL ANALYSIS

The Karush-Kuhn-Tucker (KKT) condition is a necessary condition of the optimal solutions to problems (28) and (42). To get the KKT condition, we build the Lagrangian function associated with such two problems as

$$L(\Psi, \lambda, \mathbf{v}) = \eta [\bar{R}_0^{(B,\varsigma)} + \bar{R}_0^{(P,\varsigma)}(\Psi)] - \lambda_1 [\eta \bar{R}_0^{(fh,\kappa)}(\Psi) - (1-\eta)C_0] + \sum_{l=1}^L v_l \psi_l^2 + \lambda_2 \eta - \lambda_3 (\eta - 1),$$

where $\lambda = [\lambda_1, \lambda_2, \lambda_3]^T$ and $\mathbf{v} = [v_1, \dots, v_L]^T$ are vectors composed of the Lagrangian multipliers. Let $\partial L \setminus \partial \psi_l^2 = 0$, then we have

$$(A_l + \psi_l^2 + \sigma^2)^{-1} - (B_l^{(\varsigma)} + \psi_l^2 + \sigma^2)^{-1} - \lambda_1 [(A_l^{(\kappa)} + \psi_l^2 + \sigma^2)^{-1} - (\psi_l^2)^{-1}] = 0, \quad (45)$$

where $v_l = 0$ is omitted, $A_l = \sum_{m=1}^M \frac{p_m \mu_{lm}}{1+b_m}$,

$$A_l^{(\kappa)} = \begin{cases} A_l, \kappa = \mathbf{WZ}, \\ \sum_{m=1}^M p_m \mu_{lm}, \kappa = \mathbf{P2P}, \end{cases} \quad (46)$$

and

$$B_l^{(\varsigma)} = \begin{cases} 0, \varsigma=\text{SIC}, \\ \sum_{m=1}^M \left(\sum_{m'=1, m' \neq m}^M \frac{p_{m'} u_{lm'}}{1+b_{mm'}} \right), \varsigma=\text{L}. \end{cases} \quad (47)$$

A. Small η -value Case

A small η value implies that more bandwidth is allocated to fronthaul links, then the quantization degree can be reduced. Thus the values of the diagonal elements of matrix Ψ , ψ_l^2 's, become small, leading to a high SQNR.

Consider the case where the linear reception with SIC is adopted, i.e., $\varsigma=\text{SIC}$. As analyzed above, when η value is very small, the compression noise is also very small and $A_l^{(\kappa)} \gg (\psi_l^2 + \sigma^2)$. Under this high SQNR condition, we have

$$(A^{(\kappa)} + \psi_l^2 + \sigma^2)^{-1} \ll (\psi_l^2 + \sigma^2)^{-1}, \quad (48)$$

therefore, the optimality condition (45) becomes

$$\psi_l^2 \approx \frac{\lambda_1}{1 - \lambda_1} \sigma^2, \quad (49)$$

where $\lambda_1 \in [0, 1)$. Note that (49) does not hold when $\varsigma=\text{L}$. (49) indicates that under linear reception with SIC, whatever compression scheme (either WZ coding or P2P compression) is applied at the RRHs, the optimal compression noise variance should be proportional to the background noise level when η value is small. This conclusion also suggests a simple way, referred to as uniform quantization scheme where each RRH has the same quantization noise variance, to find suboptimal solutions to problems (32), (38) and (42). The details are given as follows.

We assume $\Psi = \varrho \sigma^2 \mathbf{I}_L$. For (32), the fronthaul capacity constraint becomes a monotonically decreasing function over ϱ , thus we just need to find a certain ϱ^* , which satisfies

$$\bar{R}^{(fh, \kappa)}(\varrho^*) = (1 - \eta)C_0. \quad (50)$$

Then $\Psi = \varrho^* \sigma^2 \mathbf{I}_L$ is the output. The suboptimal algorithm with uniform quantization for problem (32) as shown in **Algorithm 3** has lower complexity than **Algorithm 1**. Actually, under certain conditions, **Algorithm 3** can achieve near optimal performance. More discussion is presented in Section VII.

With the assumption $\Psi = \varrho \sigma^2 \mathbf{I}_L$, problems (38) and (42) can be simplified to a single-variable problem of ϱ ,

$$\max_{\varrho} \frac{\bar{R}_0^{(B,\varsigma)} + \bar{R}_0^{(P,\varsigma)}(\varrho)}{\bar{R}_0^{(fh,\kappa)}(\varrho) + C_0} \quad (51a)$$

$$\text{s.t. } 0 \leq \varrho < 1, \quad (51b)$$

which can be solved via one-dimension search.

Algorithm 3 Uniform quantization algorithm for problem (32).

Input: Large-scale channel coefficients, step factor $\vartheta > 1$, and the tolerance factor ϵ .

Output: Ψ .

- 1: **Initialization:** $\varrho^{(0)} = 10^{-10}$, $\Psi^{(0)} = \varrho^{(0)} \sigma^2 \mathbf{I}_L$, and $t = 0$. Calculate $\bar{R}^{(fh,\kappa,0)}$.
 - 2: **while** $(\eta \bar{R}^{(fh,\kappa,t)} - (1 - \eta)C_0 > 0)$ **do**
 - 3: $\varrho_{min}^{(t)} = \varrho^{(t)}$ and $\varrho_{max}^{(t)} = \vartheta \varrho^{(t)}$; $t = t + 1$.
 - 4: Update $\varrho^{(t)} = \varrho_{max}^{(t-1)}$ and $\Psi^{(t)} = \varrho^{(t)} \sigma^2 \mathbf{I}_L$.
 - 5: Recalculate $\bar{R}^{(fh,\kappa,t)}$ with $\Psi^{(t)}$.
 - 6: **end while**
 - 7: Find the optimal ϱ^* in $[\varrho_{min}^{(t)}, \varrho_{max}^{(t)}]$ via one-dimensional search until $|\eta \bar{R}^{(fh,\kappa,t)} - (1 - \eta)C_0| < \epsilon$.
 - 8: **return** $\Psi = \varrho^* \sigma^2 \mathbf{I}_L$.
-

B. Large η -value case

A large η value suggests that less bandwidth is allocated to fronthaul links, so the RRHs have to increase the quantization level to meet the fronthaul capacity constraint, resulting in the larger values of $\{\psi_l^2\}_{l=1}^L$. In the case where WZ coding is adopted, i.e., $\varsigma = \text{WZ}$, when η is large, the diagonal elements of Ψ are so large that we can ignore the effect of background noise, thus

$$\bar{R}^{(P,SIC)}(\eta, \Psi) \approx \bar{R}^{(fh,WZ)}(\eta, \Psi) = (1 - \eta)C_0, \quad (52)$$

which holds regardless of what kind of WZ coding, optimal compression or uniform compression, is adopted. Therefore, when η is large enough and the linear reception with SIC is adopted, WZ coding with uniform compression can achieve near optimal performance.

Remark: Based on the aforementioned analysis, since WZ coding with uniform compression can achieve near optimal performance in both small η -value and large η -value regimes when the linear reception with SIC is adopted, we further draw a conclusion that if the linear reception with SIC is adopted, WZ coding with uniform compression can achieve the performance near to that of WZ coding with optimal compression.

VII. NUMERICAL RESULTS

In this section, we first validate the accuracy of the deterministic approximations for the ergodic SRs, and then use these deterministic results to investigate the system performance under different compression strategies. We consider a simple system where a macro BS with $N = 10$ antennas is deployed at the center, radiating over an area with a radius of 250 m. We assume the locations of RRHs and MUEs are determined respectively according to uniform distribution and SUEs are distributed uniformly within the coverage of RRHs with a radius of 50 m. The transmit power of all UEs is given as $p^{(M)} = p^{(S)} = 23$ dBm, and the noise power spectral density is -174 dBm/Hz. It is assumed that the path-loss model is described as $31.5 + 40 \log_{10}(d)$ for the SUE-to-RRH and MUE-to-RRH links and $31.5 + 35 \log_{10}(d)$ for the MUE-to-BS link, respectively, where d in meters denotes the distance [38]. The available spectrum resource is $F = 20$ MHz, which is allocated by the BS between the radio access networks and fronthaul links.

A. Validation of Accuracy of Deterministic Equivalents

We first compare Monte Carlo simulation results $R^{(B,\varsigma)} + R^{(P,\varsigma)}$ and $R^{(fh,\kappa)}$ under 10^3 trials with their analytical results $\bar{R}^{(B,\varsigma)} + \bar{R}^{(P,\varsigma)}$ and $\bar{R}^{(fh,\kappa)}$ to show the accuracy of these deterministic equivalents. We assume $N = 10$, $K = 5$, $L = 30$, $\Psi = 10^{-10} \mathbf{I}_L$, and $\eta = 0.5$. It is observed from Fig. 2 that these deterministic approximations are very close to their simulation results. Fig. 2 also shows that the linear reception with SIC achieves a larger SR than that without SIC because of less interference under the linear reception with SIC. Besides, given a fixed Ψ value, we find that $\bar{R}^{(fh,WZ)}$ is smaller than $\bar{R}^{(fh,P2P)}$, which suggests the WZ coding scheme allows a larger quantization noise variance than the P2P compression scheme when the fronthaul capacity is limited.

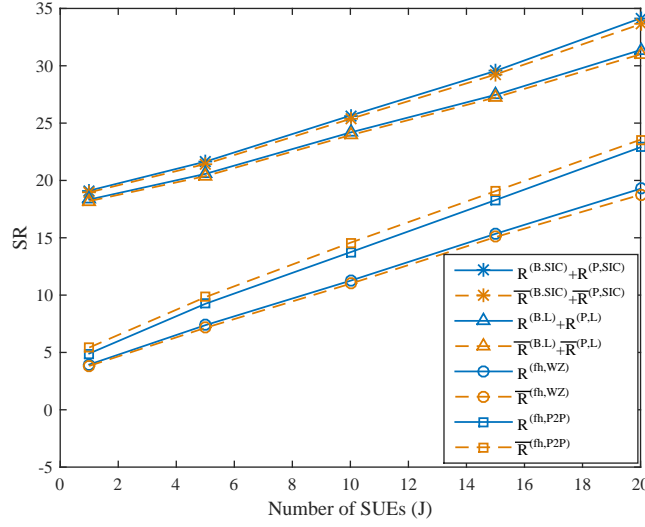


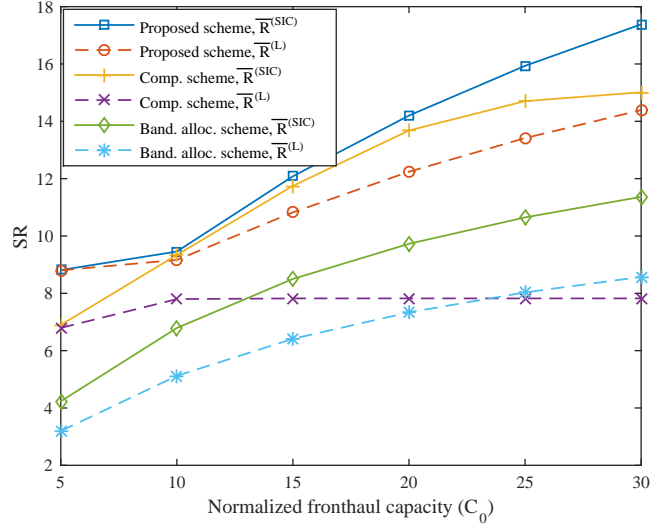
Fig. 2. Comparison of ergodic SRs and their deterministic approximations versus the number of SUEs J with $\{N = 10, K = 5, L = 30, \Psi = 10^{-10} \mathbf{I}_L, \text{ and } \eta = 0.5\}$.

B. Comparison with Other Schemes

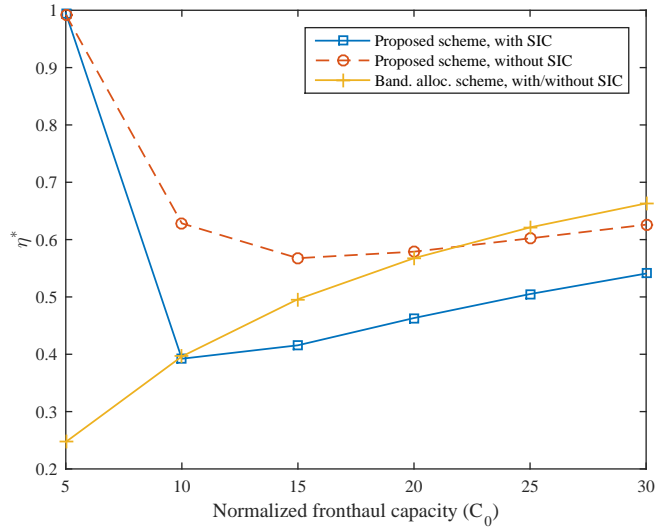
In order to show the performance of the proposed scheme, we introduce two baseline schemes:

- 1) Fix the bandwidth allocation factor η , then find the optimal compression noise matrix Ψ to maximize the achievable SR; and
- 2) fix the compression noise matrix Ψ , then find the optimal bandwidth allocation factor η to maximize the achievable SR.

We refer to such two schemes as compression scheme and bandwidth allocation scheme, respectively. For convenience of expression, we define $\bar{R}^{(L)} = \bar{R}^{(B,L)} + \bar{R}^{(P,L)}$ and $\bar{R}^{(SIC)} = \bar{R}^{(B,SIC)} + \bar{R}^{(P,SIC)}$. Fig. 3(a) depicts the achievable maximal SR versus the normalized fronthaul capacity and Fig. 3(b) presents the corresponding optimal bandwidth allocation factor η^* . Here, we set $L = 4$, $J = 4$, and $K = 2$ and adopt WZ coding. Besides, η in the compression scheme (labelled as “Comp. scheme”) is set as 0.5 and Ψ in the bandwidth allocation scheme (labelled as “Band. alloc. scheme”) is set as 10^{-13} , which is in the same order of magnitude as the background noise. From Fig. 3(a), it is observed that the proposed scheme outperforms than the two baseline schemes, no matter what decoding method, linear reception with or without SIC, is adopted. This is because the proposed scheme provides more flexibility for SR maximization. We can also find that the linear reception with SIC always achieves a higher SR than that without SIC because in the SIC scheme, the



(a)



(b)

Fig. 3. Maximal achievable SR (a) and the optimal η value (b) versus the normalized fronthaul capacity C_0 with $\{L = 4, J = 4, \text{ and } K = 2\}$.

latter-decoded user messages have less interference.

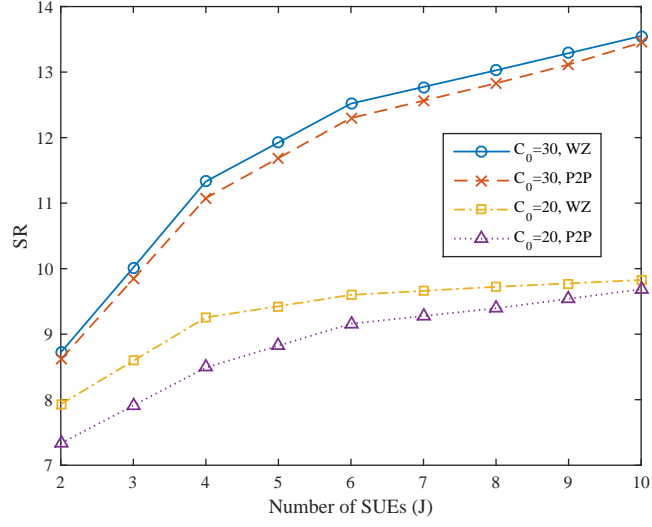
Fig. 3(b) illustrates that the optimal bandwidth allocation factor η^* increases as the normalized fronthaul capacity C_0 rises in the bandwidth allocation scheme. Typically when $C_0 \rightarrow \infty$, $\eta^* \rightarrow 0$. However, the proposed scheme does not meet such a monotonously growing trend. In the proposed scheme as C_0 increases, η^* also grows in the large C_0 -value regime because the larger normalized fronthaul capacity is, the less bandwidth fronthaul needs. But in much smaller C_0 -value regime, the fronthaul capacity is also small no matter how much bandwidth is allocated to fronthaul links, so that the achievable SR at the BBU is very small. We aim to maximize the achievable SR including the SR at the BS and that at the BBU, thus almost all bandwidth is reserved for radio access links to maximize the SR at the BS, i.e., $\eta \approx 1$.

C. Comparison of WZ Coding and P2P Compression

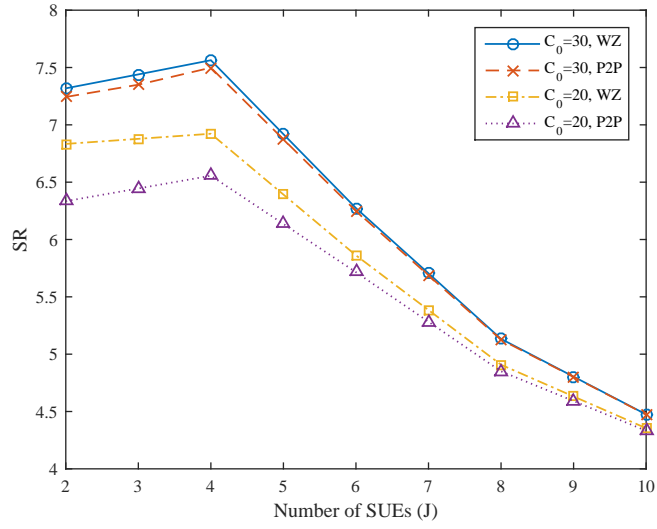
Figs. 4(a) and 4(b) present the achievable SRs $\bar{R}^{(P,SIC)}$ and $\bar{R}^{(P,L)}$ versus the number of SUEs J under different compression schemes, respectively, with $\{L = 4, K = 2, \text{ and } \eta = 0.5\}$. We observe that WZ coding always achieves a larger SR than P2P compression, because WZ coding takes advantage of the correlation of the received signals at the RRHs as side information when decompressing signals. Figs. 4(a) and 4(b) also illustrate that the achievable SRs $\bar{R}^{(P,SIC)}$ and $\bar{R}^{(P,L)}$ increase with the normalized fronthaul capacity since more bits are allowed to be transmitted to the BBU pool simultaneously. As the number of SUEs increases, the achievable SR $\bar{R}^{(P,SIC)}$ as shown in Fig. 4(a) becomes larger. However, the achievable $\bar{R}^{(P,L)}$ as shown in Fig. 4(b), first increases and then decreases because more SUEs bring more inter-user interference which hinders the growth of $\bar{R}^{(P,L)}$.

D. Comparison of Uniform Compression and Optimal Compression

Figs. 5(a) and 5(b) compare the optimal compression and uniform compression versus different η values with $\{C_0 = 30, L = 4, J = 4, \text{ and } K = 2\}$ under WZ coding and P2P compression, respectively. From Fig. 5(a), we observe that in the case of WZ coding, when the linear reception with SIC is adopted, the uniform compression can achieve near optimal performance, compared to the optimal compression. However, under the linear reception without SIC, the optimal compression shows a better performance than the uniform compression. On the other hand, in the case of P2P compression as shown in Fig. 5(b), even though the linear reception with SIC

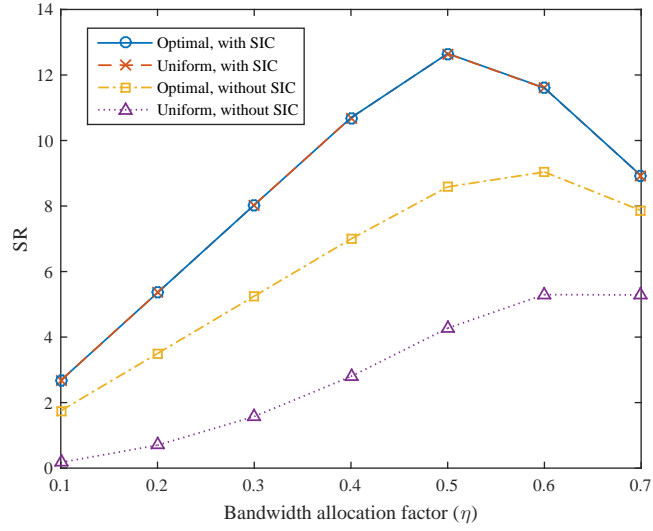


(a)

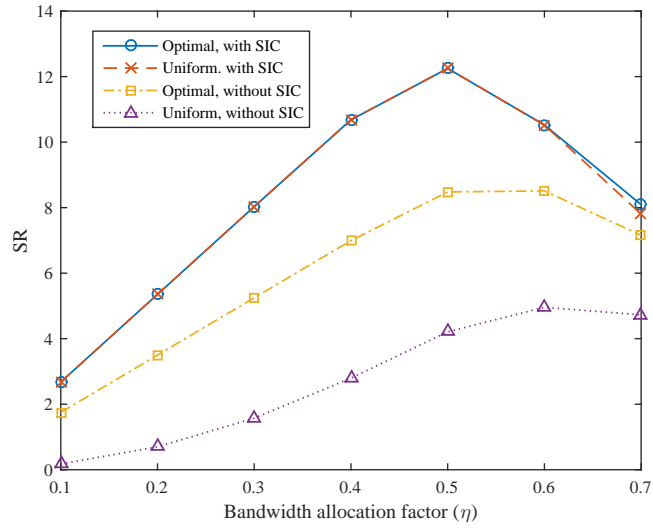


(b)

Fig. 4. (a) and (b) are the achievable SRs $\bar{R}^{(P,SIC)}$ and $\bar{R}^{(P,L)}$ versus the number of SUEs J under different compression schemes, respectively, with $\{L = 4, K = 2, \text{ and } \eta = 0.5\}$.



(a)



(b)

Fig. 5. Comparison of the optimal compression and uniform compression under (a) WZ coding and (b) P2P compression, respectively, with $\{C_0 = 30, L = 4, J = 4, \text{ and } K = 2\}$.

is adopted, the uniform compression achieves the near optimal performance only in the small η -value regime but has a suboptimal performance in the large η -value regime. Such observations prove the analysis in Section VI, i.e., the approximation in (49) holds in the condition of high SQNR. Besides, Figs. 5(a) and 5(b) also suggest that the linear reception with SIC always achieves a higher SR than that without SIC under both two cases of the optimal compression and the uniform compression.

VIII. CONCLUSION

In this work, we considered an economic solution to the challenge of limited fronthaul capacity, where the fronthaul links shared spectrum resource with radio access networks. To maximize the achievable SR in an uplink H-CRAN, we jointly optimized fronthaul compression and bandwidth allocation considering different decoding strategies and different compression schemes. Large dimensional random matrix theory was used to derive the deterministic expressions for the ergodic SR. Then, an approximation problem of the joint optimization problem was formulated, which only depended on statistical channel information. Thus the communication overhead for obtaining channel information and computational complexity were reduced significantly. The simulations results showed that WZ coding always achieved a larger SR than P2P compression at the cost of computational complexity. The linear reception with SIC had a better performance than that without SIC because the former used interference cancellation technique to improve the decoding performance, but the latter decoded each UE's message independently. Actually, to some extent, we could approximately take the achievable SRs under the two decoding strategies as the upper bound and lower bound. Besides, we also provided the performance analysis of uniform compression. Typically, when the linear reception with SIC was applied, the uniform compression with WZ coding could achieve the near optimal performance. Finally, the influence of the normalized fronthaul capacity on the optimal bandwidth allocation coefficient was analyzed. If the normalized fronthaul capacity is much smaller, almost all the bandwidth was allocated to the radio access networks. However, in the large normalized fronthaul capacity regime, the optimal bandwidth allocation coefficient, as well as the maximal achievable SR, increased with the normalized fronthaul capacity.

APPENDIX A

PROOF OF LEMMA 1

We first assume that $R^{(B,SIC)}(\sigma^2)$ is a function of σ^2 . Since $R^{(B,SIC)}(\sigma^2) = \eta R_0^{(B,SIC)}(\sigma^2)$ and $\bar{R}^{(B,SIC)}(\sigma^2) = \eta \bar{R}_0^{(B,SIC)}(\sigma^2)$, it is equivalent to validating that $R_0^{(B,SIC)}(\sigma^2) - \bar{R}_0^{(B,SIC)}(\sigma^2) \rightarrow 0$, as $N \rightarrow \infty$. The derivative of $R_0^{(B,SIC)}(\sigma^2)$ with respect to σ^2 is expressed as

$$\frac{\partial R_0^{(B,SIC)}(\sigma^2)}{\partial \sigma^2} = \frac{1}{\log 2} \left\{ \mathbb{E} [\text{tr}(\mathbf{H}\mathbf{P}^{(M)}\mathbf{H}^H + \sigma^2\mathbf{I}_N)^{-1}] - \frac{N}{\sigma^2} \right\}. \quad (53)$$

The relation between the mutual information $R_0^{(B,SIC)}(\sigma^2)$ and $\text{tr}(\mathbf{H}\mathbf{P}^{(M)}\mathbf{H}^H + \sigma^2\mathbf{I}_N)^{-1}$ can be equivalently written as [32, 39],

$$R_0^{(B,SIC)}(\sigma^2) = \frac{1}{\log 2} \int_{-\infty}^{\sigma^2} \left\{ \mathbb{E} [\text{tr}(\mathbf{H}\mathbf{P}^{(M)}\mathbf{H}^H + \omega\mathbf{I}_N)^{-1}] - \frac{N}{\omega} \right\} d\omega. \quad (54)$$

According to the random matrix theory [30], we get

$$\text{tr}(\mathbf{H}\mathbf{P}^{(M)}\mathbf{H}^H + \omega\mathbf{I}_N)^{-1} \asymp \text{tr} \left(\frac{1}{N} \sum_{k=1}^K \frac{Np_k^{(M)}\nu_k\mathbf{I}_N}{1 + e_k} + \omega\mathbf{I}_N \right)^{-1} \quad (55)$$

$$= \text{tr}(\mathbf{\Gamma}^{-1}), \quad (56)$$

where $a \asymp b$ denotes that $a - b \rightarrow 0$ as $N \rightarrow \infty$. Then, we define $\mathbf{\Sigma}_k = p_k^{(M)}\nu_k\mathbf{I}_N$ and

$$R(\sigma^2, \mathbf{x}_k) = \frac{1}{\log 2} \left[\log \left| \sum_{k=1}^K x_k \mathbf{\Sigma}_k + \sigma^2 \mathbf{I}_N \right| + \sum_{k=1}^K (x_k - \log x_k) - N \log \sigma^2 \right], \quad (57)$$

where $\mathbf{x}_k = [x_1, \dots, x_K]^T$ is a vector consisting of K variables. The derivative of $R_0^{(B,SIC)}(\sigma^2)$ with respect to σ^2 can be expressed as

$$\frac{\partial R_0^{(B,SIC)}(\sigma^2)}{\partial \sigma^2} = \frac{\partial R(\sigma^2, \mathbf{x}_k)}{\partial \sigma^2} \Big|_{x_k = \frac{1}{1+e_k}} + \sum_{k=1}^K \frac{\partial R(\sigma^2, \mathbf{x}_k)}{\partial x_k} \Big|_{x_k = \frac{1}{1+e_k}} \frac{\partial e_k}{\partial \sigma^2}. \quad (58)$$

Note that $\frac{\partial R(\sigma^2, \mathbf{x}_k)}{\partial x_k} \Big|_{x_k = \frac{1}{1+e_k}} = 0$, therefore

$$\frac{\partial R_0^{(B,SIC)}(\sigma^2)}{\partial \sigma^2} = \frac{\partial R}{\partial \sigma^2} \Big|_{x_k = \frac{1}{1+e_k}}, \quad (59)$$

which is equal to (15).

Taking the same actions on the numerator and denominator of $R_0^{(B,L)}(\eta)$, respectively, then we have

$$\log_2 |\mathbf{H}\mathbf{P}^{(M)}\mathbf{H}^H + \sigma^2\mathbf{I}_N| - \frac{1}{\log_2} \Delta_0 \rightarrow 0, \quad (60)$$

and

$$\log_2 |\mathbf{H}_{[k]} \mathbf{P}_{[k]}^{(M)} \mathbf{H}_{[k]}^H + \sigma^2 \mathbf{I}_N| - \frac{1}{\log_2} \Delta_k \rightarrow 0. \quad (61)$$

Finally, the results of (60) and (61) can be formed into $\bar{R}_0^{(B,L)}(\eta)$. Hence the proof is completed. ■

APPENDIX B

PROOF OF PROPOSITION 1

The proof of **Proposition 1** is based on [35]. We assume ω^* is the optimal solution to (39), then

$$\omega^* = \frac{f(\Psi^*, \Omega^*)}{g(\Psi^*)} \geq \frac{f(\Psi, \Omega)}{g(\Psi)}, \quad (62)$$

which implies

$$f(\Psi, \Omega) - \omega^* g(\Psi) \leq 0, \quad (63)$$

with the equality if and only if $\Psi = \Psi^*$ and $\Omega = (\Psi^* + \sigma^2 \mathbf{I}_L)^{-1}$.

On the other side, it is assumed that $(\Psi^*, \Omega^*) = \arg \max_{\Psi \in \mathcal{S}} [f(\Psi, \Omega) - \omega^* g(\Psi)]$, suggesting

$$f(\Psi, \Omega) - \omega^* g(\Psi) \leq f(\Psi^*, \Omega^*) - \omega^* g(\Psi^*) = 0, \forall \Psi \in \mathcal{S} \text{ and } \forall \Omega, \quad (64)$$

which in turn be rewritten as the following conditions:

$$\omega^* \geq \frac{f(\Psi, \Omega)}{g(\Psi)}, \forall \Psi \in \mathcal{S} \text{ and } \forall \Omega, \quad (65)$$

and

$$\omega^* = \frac{f(\Psi^*, \Omega^*)}{g(\Psi^*)}. \quad (66)$$

Therefore, the proof is completed. ■

APPENDIX C

PROOF OF PROPOSITION 2

The update rule for ω can be written as

$$\omega^{(t+1)} = \frac{f(\Psi^{(t)}, \Omega^{(t)})}{g(\Psi^{(t)})} = \omega^{(t)} - \frac{f(\Psi^{(t)}, \Omega^{(t)}) - \omega^{(t)} g(\Psi^{(t)})}{-g(\Psi^{(t)})}, \quad (67)$$

then

$$F(\omega^{(t)}) = (\omega^{(t+1)} - \omega^{(t)}) g(\Psi^{(t)}). \quad (68)$$

According to [35, Lemma 3.1-d], we have $F(\omega^{(t)}) \geq 0$. Since function $g(\Psi^{(t)}) > 0$, $\omega^{(t+1)} \geq \omega^{(t)}$ with the equality if and only if we have already been at convergence. Therefore, the sequence of $\{\omega^{(t)}\}$ is an increasing sequence, leading to a decreasing succession $\{F(\omega^{(t)})\}$. Given $F(\omega)$ is continuous over compact domain \mathcal{S} , **Algorithm 2** converges to an optimal solution. ■

REFERENCES

- [1] W. Xia, J. Zhang, T. Q. S. Quek, S. Jin, and H. Zhu, "Joint optimization of fronthaul compression and bandwidth allocation in heterogeneous CRAN," in *Proc. IEEE Global Commun. Conf. (GLOBECOM)*, Singapore, Dec. 2017, pp. 1–6.
- [2] M. Peng, Y. Li, Z. Zhao, and C. Wang, "System architecture and key technologies for 5G heterogeneous cloud radio access networks," *IEEE Network*, vol. 29, no. 2, pp. 6–14, Mar. 2015.
- [3] T. Q. S. Quek, M. Peng, O. Simeone, and W. Yu, *Cloud Radio Access Networks: Principles, Technologies, and Applications*. Cambridge Univ. Press, 2017.
- [4] H. Gao, J. Gao, Z. Shi, and T. Lv, "Throughput and energy efficiency of wireless powered multi-tier MIMO HetNets," *J. Signal Process. Systems*, vol. 90, no. 6, pp. 857–871, Jun. 2018.
- [5] J. Tang, W. P. Tay, T. Q. S. Quek, and B. Liang, "System cost minimization in cloud RAN with limited fronthaul capacity," *IEEE Trans. Wireless Commun.*, vol. 16, no. 5, pp. 3371–3384, May 2017.
- [6] M. Peng, X. Xie, Q. Hu, J. Zhang, and H. V. Poor, "Contract-based interference coordination in heterogeneous cloud radio access networks," *IEEE J. Sel. Areas Commun.*, vol. 33, no. 6, pp. 1140–1153, Jun. 2015.
- [7] M. Peng, Y. Li, J. Jiang, J. Li, and C. Wang, "Heterogeneous cloud radio access networks: A new perspective for enhancing spectral and energy efficiencies," *IEEE Wireless Commun.*, vol. 21, no. 6, pp. 126–135, Dec. 2014.
- [8] J. Tang, W. P. Tay, and T. Q. S. Quek, "Cross-layer resource allocation with elastic service scaling in cloud radio access network," *IEEE Trans. Wireless Commun.*, vol. 14, no. 9, pp. 5068–5081, Sep. 2015.
- [9] H. H. Yang, G. Geraci, and T. Q. S. Quek, "Energy-efficient design of MIMO heterogeneous networks with wireless backhaul," *IEEE Trans. Wireless Commun.*, vol. 15, no. 7, pp. 4914–4927, Jul. 2016.
- [10] H. Zhang, H. Liu, J. Cheng, and V. C. M. Leung, "Downlink energy efficiency of power allocation and wireless backhaul bandwidth allocation in heterogeneous small cell networks," *IEEE Trans. Commun.*, vol. 66, no. 4, pp. 1705–1716, Apr. 2017.
- [11] T. M. Nguyen, A. Yadav, W. Ajib, and C. Assi, "Resource allocation in two-tier wireless backhaul heterogeneous networks," *IEEE Trans. Wireless Commun.*, vol. 15, no. 10, pp. 6690–6704, Oct. 2016.
- [12] N. Wang, E. Hossain, and V. K. Bhargava, "Joint downlink cell association and bandwidth allocation for wireless backhauling in two-tier HetNets with large-scale antenna arrays," *IEEE Trans. Wireless Commun.*, vol. 15, no. 5, pp. 3251–3268, May 2016.
- [13] W. Xia, J. Zhang, S. Jin, C.-K. Wen, F. Gao, and H. Zhu, "Bandwidth allocation in heterogeneous networks with wireless backhaul," in *Proc. IEEE Global Commun. Conf. (GLOBECOM)*, Washington DC, USA, Dec. 2016, pp. 1–6.
- [14] S.-H. Park, O. Simeone, O. Sahin, and S. Shamai, "Performance evaluation of multiterminal backhaul compression for cloud radio access networks," in *Proc. CISS*, Princeton, NJ, USA, Mar. 2014, pp. 1–6.
- [15] S.-H. Park, O. Simeone, O. Sahin, and S. S. Shitz, "Fronthaul compression for cloud radio access networks: Signal processing advances inspired by network information theory," *IEEE Signal Process. Mag.*, vol. 31, no. 6, pp. 69–79, Nov. 2014.

- [16] Y. Zhou and W. Yu, "Optimized backhaul compression for uplink cloud radio access network," *IEEE J. Sel. Areas Commun.*, vol. 32, no. 6, pp. 1295–1307, Jun. 2014.
- [17] —, "Fronthaul compression and transmit beamforming optimization for multi-antenna uplink C-RAN," *IEEE Trans. Signal Process.*, vol. 64, no. 16, pp. 4138–4151, Aug. 2016.
- [18] S.-H. Park, O. Simeone, O. Sahin, and S. Shamai, "Robust and efficient distributed compression for cloud radio access networks," *IEEE Trans. Veh. Technol.*, vol. 62, no. 2, pp. 692–703, Feb. 2013.
- [19] T. X. Vu, H. D. Nguyen, T. Q. S. Quek, and S. Sun, "Adaptive cloud radio access networks: Compression and optimization," *IEEE Trans. Signal Process.*, vol. 65, no. 1, pp. 228–241, Jan. 2017.
- [20] S.-H. Park, O. Simeone, O. Sahin, and S. Shamai, "Joint precoding and multivariate backhaul compression for the downlink of cloud radio access networks," *IEEE Trans. Signal Process.*, vol. 61, no. 22, pp. 5646–5658, Nov. 2013.
- [21] —, "Inter-cluster design of precoding and fronthaul compression for cloud radio access networks," *IEEE Wireless Commun. Lett.*, vol. 3, no. 4, pp. 369–372, Aug. 2014.
- [22] O. Simeone, A. Maeder, M. Peng, O. Sahin, and W. Yu, "Cloud radio access network: Virtualizing wireless access for dense heterogeneous systems," *J. Commun. Netw.*, vol. 18, no. 2, pp. 135–149, Apr. 2016.
- [23] Y. Chi, L. Liu, G. Song, C. Yuen, Y. L. Guan, and Y. Li, "Message passing in C-RAN: Joint user activity and signal detection," in *Proc. IEEE Global Commun. Conf. (GLOBECOM)*, Singapore, Dec. 2017.
- [24] L. Liu, C. Yuen, Y. L. Guan, Y. Li, and C. Huang, "Gaussian message passing iterative detection for MIMO-NOMA systems with massive access," in *Proc. IEEE Global Commun. Conf. (GLOBECOM)*, Washington DC, USA, Dec. 2016, pp. 1–6.
- [25] Y. Zhou and W. Yu, "Approximate bounds for limited backhaul uplink multicell processing with single-user compression," in *Proc. IEEE Canadian Workshop Inf. Theory (CWIT)*, Toronto, ON, Canada, Jun. 2013, pp. 113–116.
- [26] X. Zhang and M. Haenggi, "The performance of successive interference cancellation in random wireless networks," *IEEE Trans. Inf. Theory*, vol. 60, no. 10, pp. 6368–6388, Oct. 2014.
- [27] H. Zhang, B. Wang, C. Jiang, K. Long, A. Nallanathan, and V. C. M. Leung, "Energy efficient dynamic resource allocation in NOMA networks," in *Proc. IEEE Global Commun. Conf. (GLOBECOM)*, Singapore, Dec. 2017, pp. 1–5.
- [28] H. Lin, F. Gao, S. Jin, and G. Y. Li, "A new view of multi-user hybrid massive MIMO: Non-orthogonal angle division multiple access," *IEEE J. Sel. Areas Commun.*, vol. 35, no. 10, pp. 2268–2280, Oct. 2017.
- [29] A. Beck and M. Teboulle, "Gradient-based algorithms with applications to signal recovery," *Convex Optimization Signal Process. Commun.*, pp. 42–88, 2009.
- [30] J. Zhang, C.-K. Wen, S. Jin, X. Gao, and K.-K. Wong, "Large system analysis of cooperative multi-cell downlink transmission via regularized channel inversion with imperfect CSIT," *IEEE Trans. Wireless Commun.*, vol. 12, no. 10, pp. 4801–4813, Oct. 2013.
- [31] W. Xia, J. Zhang, S. Jin, C. K. Wen, F. Gao, and H. Zhu, "Large system analysis of resource allocation in heterogeneous networks with wireless backhaul," *IEEE Trans. Commun.*, vol. 65, no. 11, pp. 5040–5053, Nov. 2017.
- [32] C.-K. Wen, G. Pan, K.-K. Wong, M. Guo, and J. C. Chen, "A deterministic equivalent for the analysis of non-gaussian correlated MIMO multiple access channels," *IEEE Trans. Inf. Theory*, vol. 59, no. 1, pp. 329–352, Jan. 2013.
- [33] J. Zhang, C.-K. Wen, S. Jin, X. Gao, and K.-K. Wong, "On capacity of large-scale MIMO multiple access channels with distributed sets of correlated antennas," *IEEE J. Sel. Areas Commun.*, vol. 31, no. 2, pp. 133–148, Feb. 2013.
- [34] W. Dinkelbach, "On nonlinear fractional programming," *Management science*, vol. 13, no. 7, pp. 492–498, Mar. 1967.

- [35] A. Zappone, E. Jorswieck *et al.*, “Energy efficiency in wireless networks via fractional programming theory,” *Found. Trends Commun. Inf. Theory*, vol. 11, no. 3-4, pp. 185–396, 2015.
- [36] Q. Li, M. Hong, H.-T. Wai, Y.-F. Liu, W.-K. Ma, and Z.-Q. Luo, “Transmit solutions for MIMO wiretap channels using alternating optimization,” *IEEE J. Sel. Areas Commun.*, vol. 31, no. 9, pp. 1714–1727, Sep. 2013.
- [37] L. Grippo and M. Sciandrone, “On the convergence of the block nonlinear gauss-seidel method under convex constraints,” *Oper. Res. Lett.*, vol. 26, no. 3, pp. 127 – 136, Apr. 2000.
- [38] M. Peng, K. Zhang, J. Jiang, J. Wang, and W. Wang, “Energy-efficient resource assignment and power allocation in heterogeneous cloud radio access networks,” *IEEE Trans. Veh. Technol.*, vol. 64, no. 11, pp. 5275–5287, Nov. 2015.
- [39] W. Hachem, P. Loubaton, J. Najim *et al.*, “Deterministic equivalents for certain functionals of large random matrices,” *Ann. Appl. Probab.*, vol. 17, no. 3, pp. 875–930, 2007.